Electronic Supplementary Information (ESI)

Engineering Heteroatom with Atomic Precision in Donor-Acceptor Covalent Triazine Frameworks to Boost Photocatalytic Hydrogen Production

Liping Guo[a], Yingli Niu[b], Haitao Xu[a], Qingwei Li[c], Shumaila Razzaque[a], Qi Huang[a]
Shangbin Jin* [a], and Bien Tan*[a]

[a] Key Laboratory of Material Chemistry for Energy Conversion and Storage, Ministry of Education, School of Chemistry and Chemical Engineering, Huazhong University of Science and Technology, Luoyu Road No. 1037, 430074, Wuhan, China.

Email:, jinsb@hust.edu.cn, bien.tan@mail.hust.edu.cn

[b]Department of Physics, School of Science, Beijing Jiaotong University, Shangyuancun No. 3, Beijing100044, China.

[c]Wuhan National Laboratory for Optoelectronics (WNLO), Huazhong University of Science and Technology, Luoyu Road No. 1037, Wuhan 430074, China.

1. Materials

3,6-dibromo-9-ethylcarbazole, 2,8-dibromodibenzothiophene, 2,8-dibromodibenzofuran, Lithium bis(trimethylsilyl)amide, terephthalonitrile, *p*-tolylboronic acid and terakis(triphenylphosphine) palladium (0) were purchased from TCI; dimethyl sulfoxide (DMSO), and acetyl chloride were purchased from Aladdin. Dioxane, tetrahydrofuran (THF), ether, N, N-dimethylformamide (DMF), potassium carbonate and triethanolamine (TEOA), dichloromethane, diatomite, methanol and ethanol were purchased from Sinopharm Chemical reagent Co., Ltd. All chemicals were used without any further purification except for THF, which was distilled to exclude residual water. Terephthalamidine dihydrochloride was synthesized following the literature method.[1]

2. The calculations of apparent quantum yield

The apparent quantum yield (AQY) was calculated according to the following equation[2]:

$$\text{AQY (\%)} = \frac{2 \times \text{number of evolved } H_2 \text{ molecules}}{\text{number of incident photons}} \times 100\%$$

$$= \frac{2 \times CN_A}{Pt\lambda/hc} \times 100\%$$

where C is the amount of H2 evolution per hour; λ is the irradiation light wavelength, NA is the Avogadro constant; h is the plank constant, c is light speed, t is the light irradiation time, and P is the incident light intensity.

3. Synthesis of Monomers

3.1 Synthesis of 3,6-dicarbaldehyde-N-ethylcarbazoled (Monomer-N)

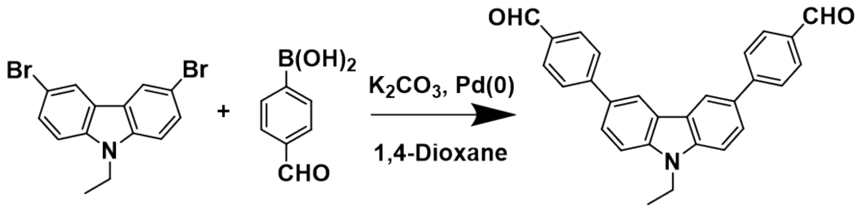

3,6-dibromo-9-ethylcarbazole (0.75 g, 2.0 mmol), *p*-tolylboronic acid (1.18 g, 8.0 mmol), potassium carbonate(1.35 g, 10 mmol) and terakis(triphenylphosphine) palladium(0.12 g, 1.0 mmol,) were mixed and then added in dioxane (16.0 mL) and water (3.6 mL). The mixture was stirred and bubbled with N_2 at room temperature for 30 min, and then stirred at 105 °C for 48 h. After cooling to room temperature, the reaction mixture was poured into water and then extracted with dichloromethane three times. Then organic phase was futher filtered with diatomite. The product was purified via recrystallization by methanol/dichloromethane. The precipitate was dried under vacuum to afford 3, 6-dicarbaldehyde-*N*-ethylcarbazole (0.42 mg, 54 %). ^{1}H-NMR (400MHz, $CDCl_3$): δ = 10.08 (s, 2H, -CHO); δ = 8.46 (s, 2H, Ar-H); δ = 8.00 (d, J = 8.0 Hz, 4H, Ar-H); δ = 7.91 (d, J = 8.0 Hz, 4H, Ar-H); δ = 7.82 (d, J = 7.2 Hz, 2H, Ar-H); δ = 7.55 (d, J = 8.0 Hz, 2H, Ar-H); δ = 4.46 (q, J = 7.2 Hz, 2H, $-CH_2-$); δ = 1.52 (t, J = 7.2 Hz, 3H, $-CH_3$); ^{13}C-NMR (75 MHz, $CDCl_3$): 191.79; 147,99; 134.65; 131.14; 130.39; 127.59; 125.72; 123.72; 119.50; 109.33; 37.99; 13.90.

3.2 Synthesis of 2,8-dicarbaldehyde dibenzothiophe (Monomer-S)

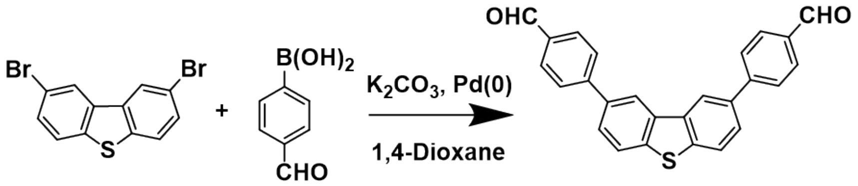

2,8-dibromodibenzothiophene (0.68 g, 2.0 mmol), *p*-tolylboronic acid (1.18 g, 8.0 mmol), potassium carbonate (1.35 g, 10 mmol) and terakis(triphenylphosphine) palladium (0.12 g, 1.0 mmol) were mixed and then added in dioxane (16.0 mL) and water (3.6 mL). The mixture was stirred and bubbled with N_2 at room temperature for

30 min, and then stirred at 105 °C for 48 h. After cooling to room temperature, the reaction mixture was poured into water and then extracted with dichloromethane three times. Then organic phase was further filtered with diatomite. The purification of product was conducted by recrystallization from methanol/dichloromethane. The precipitate was dried under vacuum to afford 2,8-dicarbaldehyde dibenzothiophe (0.64 mg, 82%). ^{1}H-NMR (400MHz, $CDCl_3$): δ = 10.11 (s, 2H, -CHO); δ = 8.48 (s, 2H, Ar-H); δ = 8.03 (d, J = 8.0 Hz, 4H, Ar-H); δ = 8.00 (d, J = 8.8 Hz, 2H, Ar-H); δ = 7.91 (d, J = 8.0 Hz, 4H, Ar-H); δ = 7.79 (d, J = 7.2 Hz, 2H, Ar-H); ^{13}C-NMR (75 MHz, $CDCl_3$): 191.87; 146.79; 140.30; 136.63; 135.30; 130.43; 127.92; 126.48; 123.56; 120.39.

3.3 Synthesis of 2,8-dicarbaldehyde –dibenzofuran (Monomer-O)

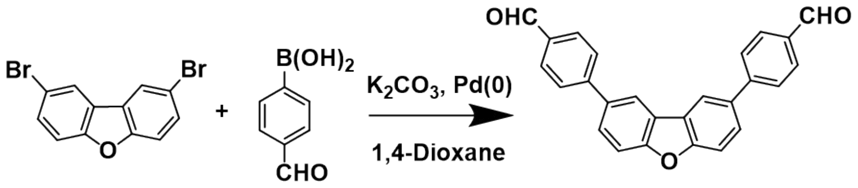

2,8-dibromodibenzofuran (0.63 g, 2.0 mmol), *p*-tolylboronic acid(1.18 g, 8.0 mmol) , potassium carbonate(1.35 g, 10 mmol) and terakis(triphenylphosphine) palladium(0.12 g, 1.0 mmol,) were mixed and then added in dioxane (16.0 mL) and water (3.6 mL). The mixture was stirred and bubbled with N_2 at room temperature for 30 min, and then stirred at 105 °C for 48 h. After cooling to room temperature, the reaction mixture was poured into water and then extracted with dichloromethane three times. Then organic phase was futher filtered with diatomite. The purification of product was conducted by recrystallization with methanol/dichloromethane. The precipitate was dried under vacuum to afford 2,8-dicarbaldehyde dibenzothiophe (0.57 mg, 76%). ^{1}H-NMR (400

MHz, $CDCl_3$): δ = 10.10 (s, 2H, -CHO); δ = 8.28 (s, 2H, Ar-H); δ = 8.02 (d, J = 8.0 Hz, 4H, Ar-H); δ = 7.87 (d, J = 8.4 Hz, 4H, Ar-H); δ = 7.79 (d, J = 8.8 Hz, 2H, Ar-H); δ = 7.71 (d, J =8.4 Hz, 2H, Ar-H); ^{13}C-NMR (75 MHz, $CDCl_3$): 191.89; 147,10; 135.19; 135.13; 130.40; 127.91; 127.21; 124.81; 119.68; 112.39.

3.4 Synthesis of 2,8-dicarbaldehyde -9H-fluorene (Monomer-C)

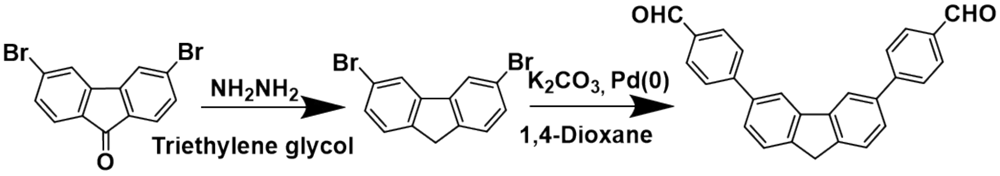

The first step was followed by the literature.[3] The second step was synthesized as following: 2,8-dibromo-*9H*- fluorene (0.63 g, 2.0 mmol), *p*-tolylboronic acid (1.18 g, 8.0 mmol), potassium carbonate (1.35 g, 10.0 mmol) and terakis (triphenylphosphine) palladium (0.12 g, 1 mmol,) were mixed and then added in toluene (16.0 mL) and water (3.6 mL). The mixture was stirred and bubbled with N_2 to purge O_2 for 30 min, and then stirred at 105 °C for 48 h. After cooling, the reaction mixture was poured into water and then extracted with dichloromethane for three times. Then organic phase was futher filtered through diatomite. The purification of product was conducted by recrystallization from petroleum ether and dichloromethane. The precipitate was dried under vacuum to afford 2,8-dicarbaldehyde dibenzothiophe (0.35 mg, 47%). ^{1}H-NMR (400MHz, $CDCl_3$: ppm): δ = 10.09 (s, 2H, -CHO); δ = 8.12 (s, 2H, Ar-H); δ = 8.00 (d, J = 8.40 Hz, 4H, Ar-H); δ = 7.87 (d, J = 8.00 Hz, 4H, Ar-H); δ = 7.69 (d, J =8.00 Hz, 2H, Ar-H); δ = 7.63 (d, J = 6.8 Hz, 2H, Ar-H); ^{13}C-NMR (75 MHz, $CDCl_3$): 191.95; 147,49; 143.96; 142.15; 138.84; 135.21; 130.35; 127.85; 126.55; 125.69; 118.86.

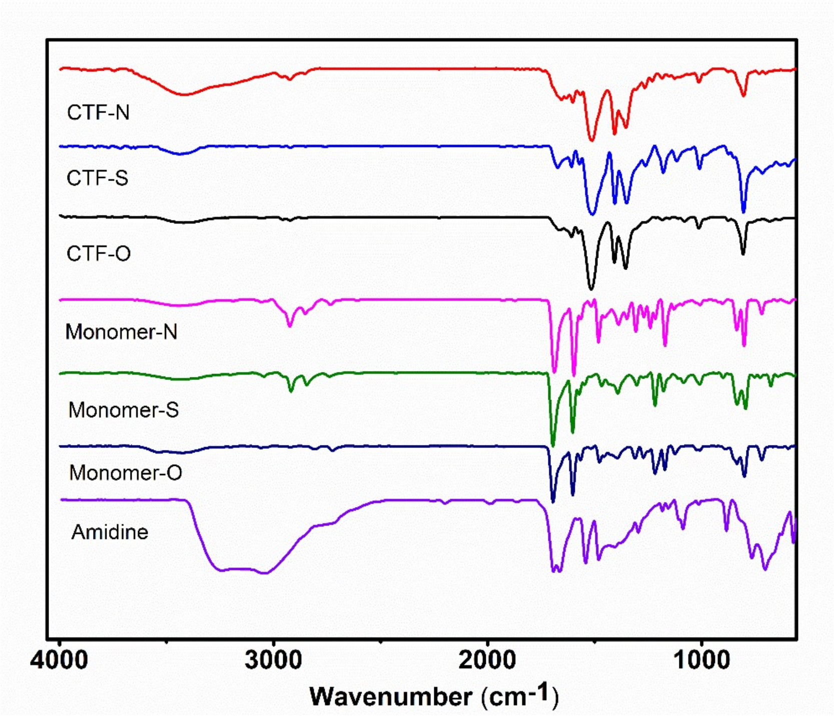

Figure S1. FT-IR of CTFs and monomers.

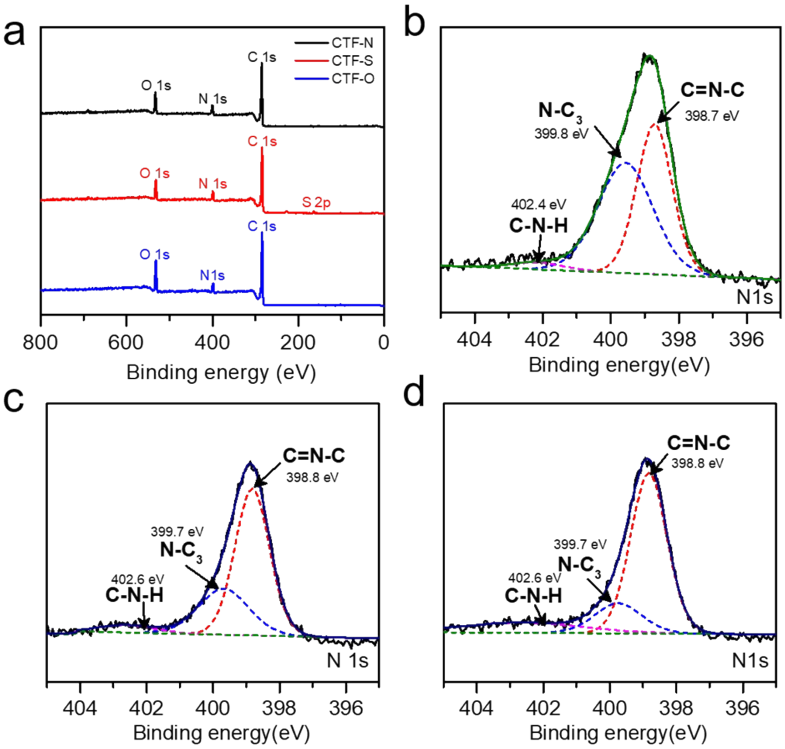

Figure S2. The survey XPS of CTFs (a); and high-resolution spectra of N 1s for CTF-N (b), CTF-S (c) and CTF-O (d).

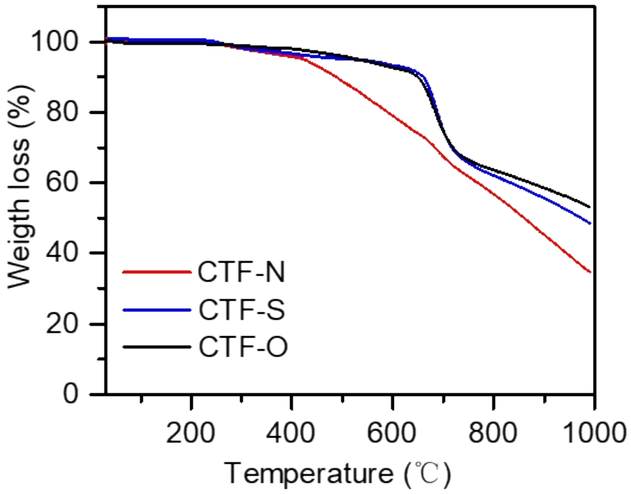

Figure S3. Thermogravimetric analysis of CTFs. Compared with CTF-S and CTF-O, CTF-N starts to lose weight at lower temperature because of the decomposition of ethyl groups in CTF-N.

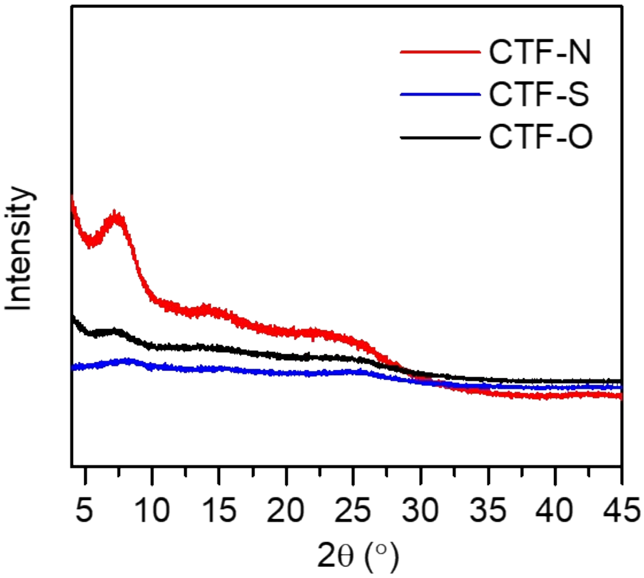

Figure S4. Powder X-ray diffraction pattern of CTF samples.

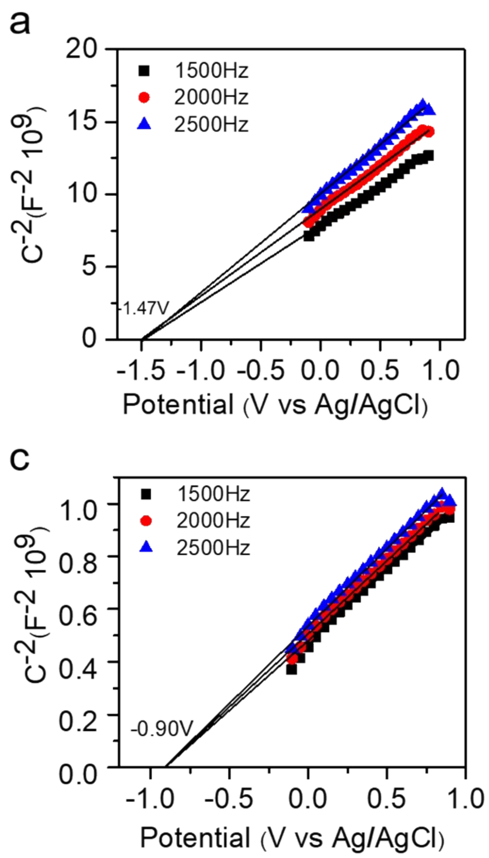

Figure S5. Mott-Schottky plots of (a) CTF-N, (b) CTF-S and (c) CTF-O samples.

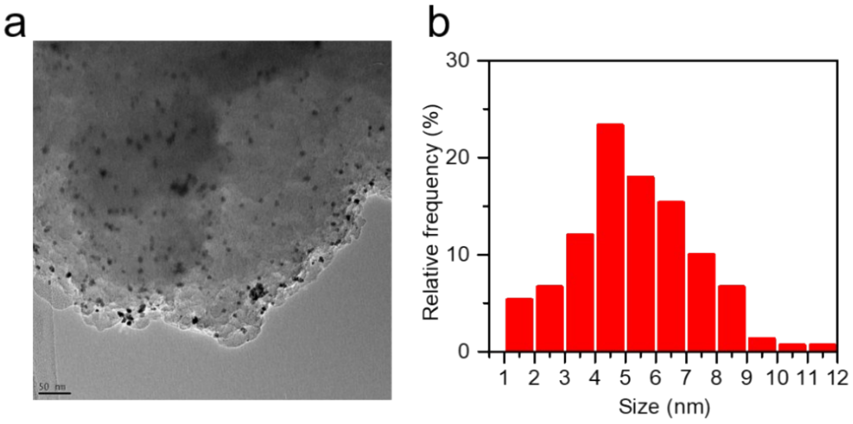

Figure S6. (a) High-resolution TEM image of CTF-N sample after loading Pt nanopartiles (the image indicates the Pt nanopartilces are uniformly distributed among CTF-N matrix); (b) The caluclation of the size distribution of Pt nanoparitlces in CTF-N.

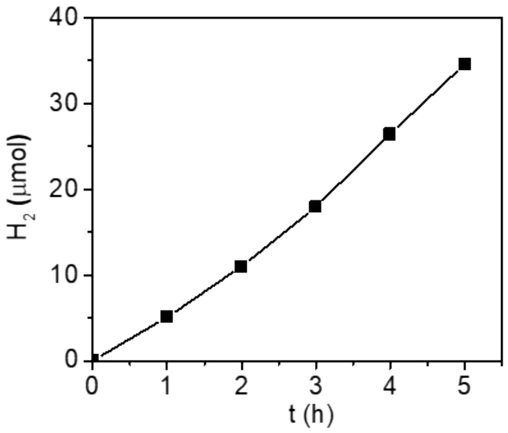

Figure S7. H_2 evolution of *g*-C_3N_4 under visible light irriadation. *g*-C_3N_4 was prepared according to the literature method [4] and the photocatalytic hydrogen evolution was measured under the identical condition with CTFs.

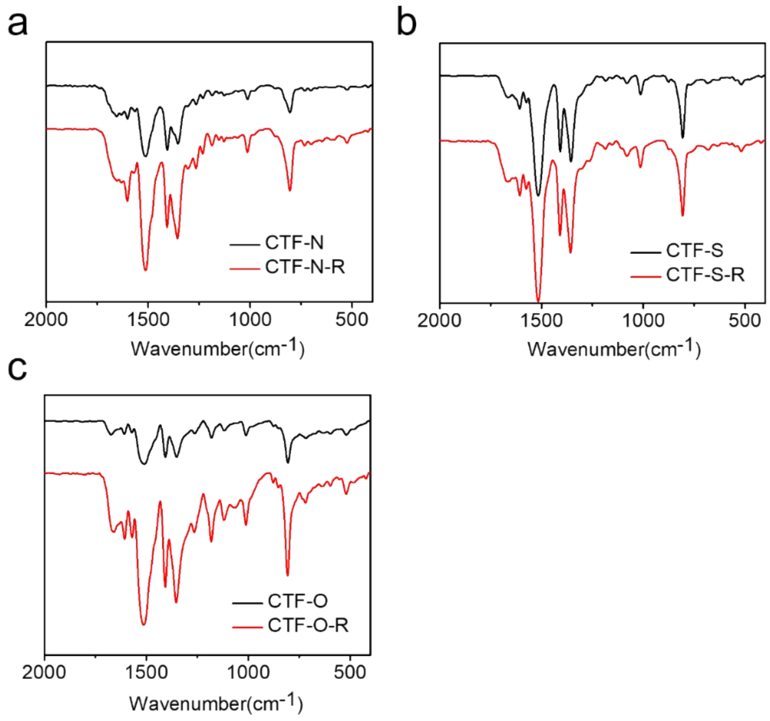

Figure S8. FT-IR spectra of corresponding CTF samples before (CTF-N, CTF-S and CTF-O) and after (CTF-N-R, CTF-S-R, CTF-O) photocatalytic process (The results indicate the structures are stable and intact after photocatalysis).

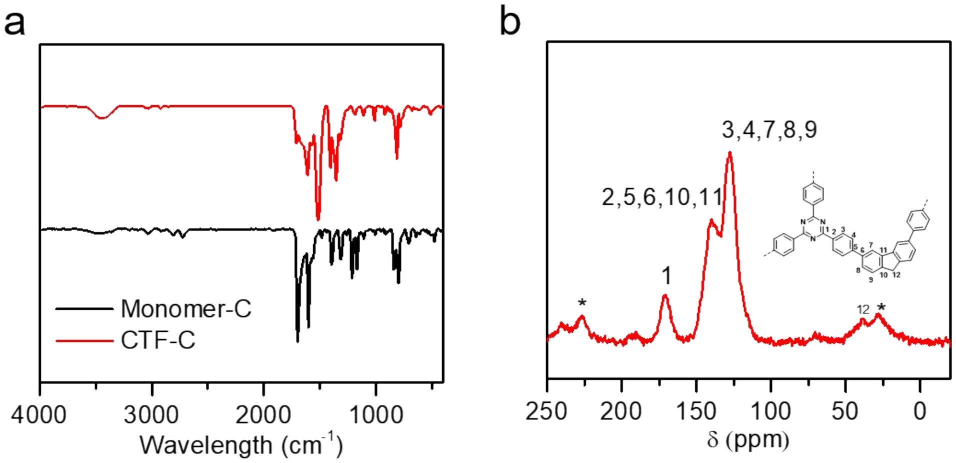

Figure S9. (a) FT-IR of CTF-C and monomer-C; (b) ^{13}C-NMR spectrum of CTF-C.

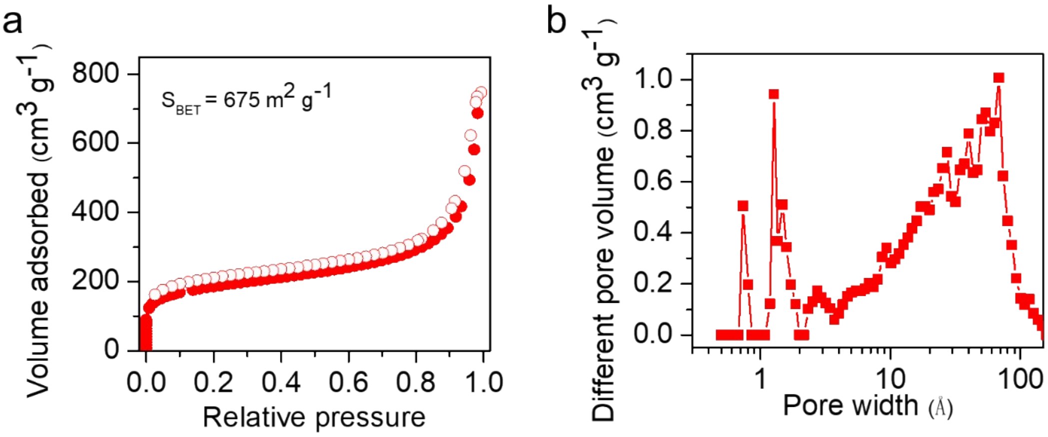

Figure S10. (a) Nitrogen sorption isotherm curve of CTF-C; (b) corresponding pore size distributions of CTF-C.

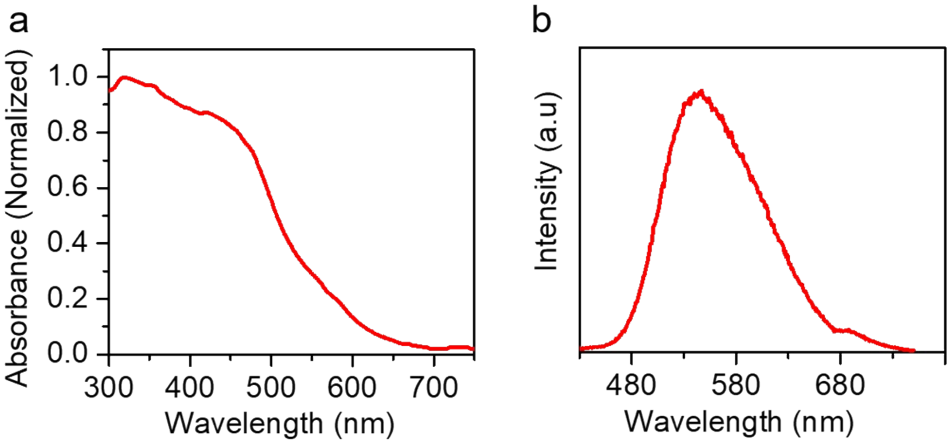

Figure S11. (a) UV-Vis spectrum of CTF-C; (b) Steady-state PL spectra of CTF-C.

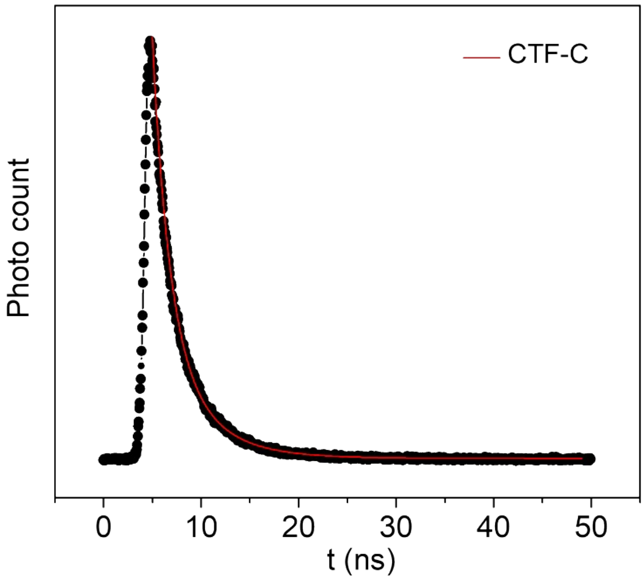

Figure S12. Time-resolved fluorescence decay profile of CTF-C sample.

Table S1.Summary of the elemental analysis results of CTFs

Samples	C (%)	H (%)	N (%)	S (%)
CTF-N[a]	81.3	3.6	15.1	/
CTF-N[b]	74.9	4.5	14.0	/
CTF-S[a]	78.5	3.4	13.1	5.0
CTF-S[b]	71.0	3.8	12.4	4.3
CTF-O[a]	80.5	3.5	13.4	/
CTF-O[b]	73.5	3.9	12.3	/
CTF-C[a]	82.8	3.7	13.5	/
CTF-C[b]	72.8	4.0	11.9	/

[a] Theoretical elemental content calculated based on infinite network structures;

[b] The average elemental content of twice measurements.

Table S2. Theoretical calculation of corresponding energy levels of building blocks in CTFs

Building blocks	HOMO (eV)	LUMO (eV)	Band gap (eV)
1,3,5-triazine	-7.74	-1.77	5.97
Carbazole	-5.55	-0.95	4.60
Dibenzothiophe	-6.03	-1.25	4.78
Dibenzofuran	-6.26	-1.23	5.03

Table S3. Summary of photoluminescence lifetimes and theoretical calculation of band gaps and the energy levels

Sample	τ (ns)	Bandgap[a] (eV)	HOMO[b] (eV)	LUMO[c] (eV)	E_{vacuum}[d] (eV)	$E_{solution}$[e] (eV)	HOMO[f] (eV)	LUMO[g] (eV)
CTF-N	0.36 (99.99%) 3.18 (0.01%)	2.17	0.90	-1.27	3.11	2.88	-5.51	-2.19
CTF-S	0.61 (99.57%) 3.64 (0.43%)	2.47	1.68	-0.79	3.37	3.21	-5.90	-2.24
CTF-O	0.89 (75.12%) 5.44 (24.88%)	2.67	1.97	-0.70	3.57	3.38	-6.09	-2.21

[a] Experimental optical band gaps of CTFs were calculated by Tauc-plot; [b] The experimental HOMO energy level of CTFs were approximately considered as the difference between band gap and LUMO value; [c] The experimental LUMO energy level of CTFs were obtained from Mott-Schottky; [d] The vertical excited energy of CTF in vacuum according TDDFT calculation; [e] The vertical excited energy of CTF in solution according TDDFT calculation based Polarizable Continuum Model (PCM); [f] The calculated theoretical HOMO value of CTFs; [g] The calculated theoretical LUMO value of CTFs.

Due to solvent effects, the excited energies of the molecules are lower in solution than in vacuum.

Table S4. Photocatalytic performance of literature reported conjugated porous polymers.

Catalyst	Condition	Amount of catalyst (mg)	Hydrogen evolution rate (μmol h^{-1})	AQY (%)	Ref.
Planarized fluorine-type polymer	>420 nm; MeOH / TEA	25	37	7.2 (420 nm)	5
Solution-Processable Polymer	>420 nm; MeOH / TEA	40	22	0.56 (420 nm)	6
Conjugated polybenzodiazoles	>420 nm; TEOA 3 wt% Pt	50	116	4.01 (420 nm)	7
CMPs	>420nm TEA	100	17	/	8
PyBT-2	>420nm TEOA	100	30	/	9
N_3-COF	>420 nm TEOA 3wt%Pt	5	9	0.45 (450 nm)	10
TFPT-COF	>420 nm; TEOA	10	20	2.2	11
Phenyl-triazine oligomers	>400 nm TEOA 2.2 wt%Pt pH = 7.0	10	11	9.9 (400 nm)	12
CTF-2	>420 nm TEOA 3 wt% Pt	25	7	1.6 (420 nm)	13
CTF-S_{10}	>420 nm TEOA 1 wt% Pt	20	40	/	14
CTF-1-100W	>420 nm TEOA 2.01 wt% Pt	50	275	6 (420 nm)	15

CTF-N	**>420 nm** **TEOA** **~2 wt%Pt**	**50**	**538**	**4.07 (420 nm)**	**This work**

References

1 K. Wang, L. M. Yang, X. Wang, L. Guo, G. Cheng, C. Zhang, S. Jin, B. Tan, A. Cooper, *Angew. Chem. Int. Ed.,* 2017, 56, 14149-14153.

2 X. Zhang, B. Peng, S. Zhang, T. Peng, *ACS Sustain. Chem. Eng.,* 2015, 3, 1501-1509.

3 Y. Song, W. Xu, D. Zhu. *Tetrahedron Lett.,* 2010, 51, 4894-4897.

4 L. Lin, H. Ou, Y. Zhang, X. Wang, *ACS Catal.,* 2016, 6, 3921−3931.

5 R. Sprick, B. Bonillo, R. Clowes, P. Guiglion, N. Brownbill, B. Slater, F. Blanc, M. Zwijnenburg, D. Adams, A. Cooper, *Angew. Chem. Int. Ed.,* 2016, 128, 1824-1828.

6 D. J. Woods; R. S. Sprick; C. L. Smith; A. J. Cowan, A. I. Cooper, *Adv. Energy Mater.,* 2017, 7, 1700479.

7 G. Zhang, Z.A. Lan, X. Wang, *Angew. Chem. Int. Ed.,* 2016, 55, 15712-15727.

8 R. Sprick, J. X. Jiang, B. Bonillo, S. Ren, T. Ratvijitvech, P. Guiglion, M. Zwijnenburg, D. Adams, A. Cooper, *J. Am. Chem. Soc.,* 2015, 137, 3265-3270.

9 Y. Xu, N Mao, C. Zhang, X. Wang, J. Zeng, Y. Chena, F. Wang, J. X. Jiang, *Appl. Catal. B-Environ.,* 2018, 228, 1-9.

10 V. S. Vyas, F. Haase, L. Stegbauer, G. Savasci, F. Podjaski, C. Ochsenfeld, B. V. Lotsch, *Nat. Commun.,* 2015, 6, 8508.

11 L. Stegbauer, K. Schwinghammer, B. V. Lotsch, *Chem. Sci.,* 2014, 5, 2789-2793.

12 K. Schwinghammer, S. Hug, M. Mesch, J. Senkerd, B. V. Lotsch, *Energ. Environ. Sci.,* 2015, 8, 3345-3353.

13 C. B. Meier, R. S. Sprick, A. Monti, P. Guiglion, J. S. M. Lee, M.A. Zwijnenburg, A. I. Cooper. *Polymer,* 2017, 126, 283-290.

14 L. Li, W. Fang, P. Zhang, J. Bi, Y. He, J. Wangc, W. Su, *J. Mater. Chem. A,* 2016, 4, 12402-12406.

15 J. Xie, S. A. Shevlin, Q. Ruan, S. A. Moniz, Y. Liu, X. Liu, Y. Li, C. C. Lau, Z. X. Guo, J. Tang, *Energ. Environ. Sci.,* 2018, 11, 1617-1624.